Online Appendix

Expanded Methods

Atherosclerosis

Male *Apoe*$^{-/-}$ mice were injected IP with TRAF-STOP 6877002 (n=13 and n=12), TRAF-STOP 6860766 (n= 12 and n= 11) at 10 μmol/kg/day, or vehicle (PBS, 0.05% Tween 80, 5% DMSO) (n=15 and n=11) for 6 weeks, starting at the age of 12 or 22 weeks, and were fed a normal chow diet throughout the experiment. Mice were then sacrificed and the arterial tree was perfused. The aortic arch and its main branch points were excised, fixed overnight, and embedded in paraffin. Longitudinal sections of the aortic arch and transversal sections of the aortic root were analyzed for plaque extent and morphology as described previously (1). For histological analyses, the aortic arch was cut in 40 longitudinal sections (4 μm) and four sections (20 μm apart) were stained with hematoxylin and eosin. The aortic arch region was defined as the aortic root to approximately 1.5 mm caudal from the left subclavian artery branch point. The main branch points (the brachiocephalic trunk, left common carotid artery and left subclavian artery) were also included into the measurements. Plaque area, excluding the underlying media, was determined for each individual plaque, and the sum of all plaques in the aortic arch was used to determine total atherosclerotic plaque area per aortic arch. This was done for 4 sections (20 μm apart), and the mean was calculated to determine total plaque area in the aortic arch for 1 mouse. Plaques were classified as intimal xanthoma, pathological intima thickening or fibrous cap atheroma. An intimal xanthoma (IX) is defined by a small lesion consisting of foam cells in which no extracellular lipid accumulation can be detected. A pathological intimal thickening (PIT) is defined as a larger lesion that mainly consists of macrophage foam cells, but contains

small extracellular lipid pools and the first matrix depositions. A fibrous cap atheroma (FCA) is defined as an advanced atherosclerotic lesion with a clear fibrous cap and necrotic cores (extracellular lipid accumulation, cholesterol crystals and/or calcification). For phenotypic analysis, immunohistochemistry (IHC) was performed for CD3 (Dako), Mac-3 (BD Bioscience), Ly6G (BD Bioscience), α-SMA (Sigma-Aldrich) and ki67 (Abcam). Sirius red staining was performed as described (1). Sections were analyzed using a Leica DM6000 microscope and morphometric analyses were performed using the Las4.0 software (Leica) or Image J. Plasma cholesterol levels were measured enzymatically (Roche).

rHDL-6877002 treatment of atherosclerosis

Male *Apoe*$^{-/-}$ mice were injected IV with rHDL-6877002 (10 μmol/kg; n=8) or rHDL (n=8) or NaCl 0.9% (n=8) twice a week for 6 weeks from the age of 12 weeks, and were fed a normal chow diet throughout the experiment. Atherosclerosis was analyzed as described above.

Flow cytometry

At sacrifice, blood was obtained from the heart in EDTA-coated syringes. Erythrocytes were lysed by incubation with a hypotonic buffer (8.4 g of NH_4Cl and 0.84 g of $NaHCO_3$ per liter of distilled water). Spleens were weighed and pushed through a 70 μm cell-strainer, spun down, resuspended in red cell lysis buffer for 4 minutes, and then inactivated using serum containing media, spun down and resuspended in 1000 μL serum containing media per 100 mg of spleen tissue. Cells were run through a 70μm strainer, and twice spun down and resuspended in serum containing media.

Non-specific antibody binding was prevented by pre-incubation with a Fc-receptor blocking antibody (eBioscience). The following antibodies were used: F4/80-PE-Cy7 (clone BM8, BioLegend); CD11b-PerCP/Cy5.5 (clone M1/70, BioLegend); CD11c–APC (clone N418, BioLegend); CD45-brilliant violet 510 (clone 30-F11, BioLegend); Ly-6C–PE (clone AL-21, BD Biosciences); Ly6C-FITC (clone AL-21), BD Biosciences); NK1.1-eFluor 450 (clone PK136, eBioscience); NK1.1-PE (clone PK136, BD Biosciences); CD49b-eFluor 450 (clone DX5, eBioscience); CD45R-eFluor450 (clone RA3-6B2, eBioscience); Ly-6G-Pacific Blue (clone 1A8, BioLegend); Ly-6G-PE (clone 1A8, BD Biosciences); CD3-PE (clone 17A2; BioLegend), CD3-FITC (eBioscience), CD4-PeCy7 (BD bioscience), CD8-PE (eBioscience); CD19-PE (clone 1D3, BD Bioscience), c-kit (clone 2B8, BioLegend), CD150 (clone TC15-12F12.2, BioLegend), CD16/32 (clone 93, BioLegend), CD11a (clone M17/4, BioLegend), IL7rα (clone A7R34, BioLegend), Sca-1 (clone D7, eBioscience), TER119 (clone TER-119, BioLegend), CD135 (clone A2F10, Biolegend), CD40 (clone 3/23, Biolegend). The antibody dilutions ranged from 1:100 to 1:1000. Cells were analyzed on a FACSCanto II flow cytometer (BD Bioscience).

Toxicity studies

At sacrifice, absolute peripheral blood counts were determined using a scil Vet abc Plus+ haematology analyzer (Scil Animal Care Company B.V.). Autopsy was performed and organs (including lung, liver, heart, kidneys, bladder, genitals, pancreas, lymph nodes, spleen, salivary glands, stomach, small and large intestines) were analyzed macroscopically and microscopically by an animal pathologist (M.G.). For histological analysis, organs were fixed in paraformaldehyde (4%, overnight), sectioned at 4 µm, and stained with hematoxylin and eosin or the indicated antibodies, as described before. Sirius red staining was performed to determine collagen content.

Fasting insulin levels (Mercodia), AST (Biomatik), ALT (Biomatik), leptin (Crystalchem) and adiponectin (Assaypro) were determined by ELISA. Fasting glucose levels were determined by a Glucose Assay Kit (Abcam) according to the manufacturer's protocol. The homeostasis model assessment of insulin resistance was calculated. ELISA was used to determine the plasma levels of IgM (Bender MedSystems), IgG (Bender MedSystems), and anti-MOG IgG (AnaSpec).

Intravital microscopy

Intravital microscopy of the carotid artery was performed in *Cx3cr1egfp/Apoe*$^{-/-}$ mice (n=5 vehicle, n=7 6877002, n=8 6860766) that were fed a 0.15% cholesterol diet for 6 weeks as previously described (1). Mice received a single IP injection of the TRAF-STOP or vehicle. A PE-conjugated antibody to Ly6G (1A8, 1 µg) was instilled via a jugular vein catheter 5 minutes prior to recording. After recording of neutrophil and monocyte adhesion, rhodamine 6G was administered to visualize all adherent leukocytes. Intravital microscopy was performed using an Olympus BX51 microscope equipped with a beam splitter to enable synchronized dual-channel recording, a Hamamatsu 9100-02 EMCCD camera, and a 10x saline-immersion objective. Olympus cell software was used for image acquisition and analysis.

Two-photon laser scanning microcopy of whole-mount carotid arteries

6-8 weeks old *Apoe*$^{-/-}$ mice received a 0.15% cholesterol diet for 6 weeks. Carotid arteries were explanted and treated with TRAF STOP 6877002 (10 µmol/L) or control. Treated vessels were mounted on glass micropipettes in a home built arteriography chamber. CD31 and VCAM-1 expression were analyzed using CD31 (eBioscience) and VCAM-1 (Biolegend) antibodies. The mounted carotid arteries were visualized using a LeicaSP5IIMP two-photon laser scanning

microscope with a pre-chirped and pulsed Ti:Sapphire Laser (Spectra Physics MaiTai Deepsee) tuned at 800nm and a 20×NA1.00 (Leica) water dipping objective. Image acquisition, processing, and quantification were performed using LasX software including the 3D analysis package (Leica).

In vitro bone marrow derived macrophages

Bone marrow (BM) cells were isolated from C57Bl6 mice, *CD40*$^{-/-}$, *CD40*$^{+/+}$, *CD40-Traf wild type (Twt)*, *CD40-T2/3/5*$^{-/-}$ or *CD40-T6*$^{-/-}$ and cultured in RPMI supplemented with 15% L929-conditioned medium to generate BM-derived macrophages (BMDMs). BMDMs were activated by the agonistic CD40 antibody FGK45 (25 µg/ml, Bioceros BV) for 6 hours. CCL-2 was determined by ELISA (eBioscience) according to the manufacture's protocol.

Quantitative PCR

RNA was isolated from BM-derived macrophages, THP1 cells, Jurkat cells, CA46 cells, HUVECs and reverse transcribed using an iScript cDNA synthesis kit (Bio-Rad). Quantitative (q)PCR was performed with a SYBR Green PCR kit (Applied Biosystems) on a ViiA 7 real-time PCR system (Applied Biosystems). Primer sequences are available upon request.

Migration assay

Human blood monocytes were isolated from buffy coats of healthy donors by Ficoll gradient and CD14-coated beads. The procedure was approved by the local human experimental committee. The human endothelial cell (EC) line hCMEC/D3 was grown in endothelial cell basal medium-2 supplemented with hEGF, hydrocortisone, GA-1000, FBS, VEGF, hFGF-B, R3-IGF-1, ascorbic

acid and 2.5 % fetal calf serum (EGM-2). hCMEC/D3 cells were grown to confluence in 96-well plates. Monocytes or EC were incubated with the vehicle or 6877002 or 6860766 at 10 µM for 1 hour, after which a CD40 stimulating antibody was added at 30 µg/ml for 10-12 hours (G28.5, Bioceros, Utrecht, the Netherlands). After extensive washing, monocytes (7.5 10^5 cells/ml) were added to EC monolayers and the number of migrated monocytes was assessed after 4 hours. Migrated cells were quantified by counting per field-of-view. From one experiment, five fields were analyzed. Movies were generated using VirtualDub**.**

Chemotaxis assay

Chemotaxis of macrophages was assessed using 24-well Transwell migration chambers (Costar; Corning) with a pore size of 5 µm. BM-derived macrophages (5×10^4) were treated with TRAF-STOP or vehicle and FGK-45 or isotype control (as described above) and added to the chamber. Complete medium, including 100 ng/ml CCL2 (R&D Systems), was added to the lower chambers and migration was performed at 37°C for 4 hours. Non-migrated cells were removed from the membranes, and migrated cells were fixed with PFA and stained with toluidine blue. Membranes were cut out of inserts and mounted onto slides in immersion oil. The number of migrated cells was counted on five randomly chosen fields of each membrane.

In vitro lipid uptake, phagocytosis and efferocytosis

BMDMs were obtained as described above. BMDMs were treated with TRAF-STOPs and subsequently activated with the agonistic CD40 antibody FGK45 (25 µg/ml, Bioceros BV) for 6 hours. After 24 hours, BMDMs were labeled with CD36-APC (BioLegend) and expression was analyzed using flowcytometry. Oil Red O staining (0.3% in 60% isopropanol, Sigma) was

performed to determine lipid accumulation. For phagocytosis experiments, fluorescently labeled latex beads were incubated with the BMDMs, as described above, and uptake was analyzed by flowcytometry. For oxLDL uptake studies, TRAF-STOP-treated BMDMs were incubated with 12.5 μg/ml Dil-oxLDL (Sanbio, Uden, The Netherlands) for 6 hours. Uptake was assessed by flow cytometry after residual DiI-oxLDL was washed away and expressed as mean fluorescent intensity. For efferocytosis studies, BMDMs were fluorescently labeled using Celltrace CSFE Cell Proliferation Kit (Invitrogen) according to manufacturer's instructions. Next, apoptosis was induced by adding hydrogen peroxide. After 24 hours, the cells were washed and the apoptotic cells were added to the TRAF-STOP treated BMDMs. After 6 hours, uptake of apoptotic cells was analyzed by flowcytometry.

Cell cultures

THP-1, Jurkat and CA46 cells were cultured in RPMI1640 medium (Invitrogen) containing 10% FCS, Glutamate, and penicillin/streptavidin. HUVECs were cultured in M199 (GIBCO Invitrogen) with 100 U/ml Penicillin/Streptomycin (P/S), 20% heat-inactivated FCS, 0.05μg/ml of heparin (Sigma), 2mM L-Glutamine (Invitrogen) and 25μg/ml Endothelial Cell Growth Supplement (ECGS, Sigma). HUVECs were used between passage 1 and 3 for experiments. THP-1 cells were differentiated into macrophages by 48 hours PMA (50μg/mL) stimulation.

After 1 hour incubation with TRAF-STOP 6877002, 6860766 or vehicle, THP-1 cells were activated with LPS (10 ng/mL), Jurkat cells were activated with CD3/CD28 Dynabeads (ThermoFisher), CA46 cells with the agonistic G28.5 (10 μg/mL) CD40 antibody (Bioceros) and R848 (2.5 μg/mL), HUVECs with G28.5 (10 μg/mL) and TNF (10 ng/mL) for 6 hours. After the experimental procedure, cells were lysed and RNA was isolated.

Western blot

BMDMs were cultured as described above and incubated with vehicle of TRAF-STOP at 10 µM 1 hour our prior to stimulation with FGK45 (30 ug/ml, Bioceros BV). BMDM were stimulated for 10 minutes or 24 hours and subsequently lysed in RIPA lysis buffer. Protein concentrations were determined using the Pierce BCA Protein Assay Kit (Thermo Scientific). Equal amounts of protein samples were loaded on a SDS polyacrylamide gel and transferred to a nitrocellulose membrane (Bio-Rad). After blocking with 5% BSA in PBS containing 0.05% Tween-20, blots were incubated overnight with the indicated antibodies; pTAK, NF-κBp65, pNF-κBp65 αTubulin, β-actin and NF-κB2 antibodies were from Cell Signaling Technology, pERK and ERK antibodies were from Santa Cruz. Blots were then washed and incubated with the appropriate HRP-conjugated secondary antibody (1:5000; DAKO) and visualized using the ECL substrate kit (Thermo Scientific).

Transcriptomics

BMDMs of C57Bl6 mice (n=3) were pre-incubated with vehicle or TRAF-STOP for 1 hour and subsequently activated by the agonistic CD40 antibody FGK45 (25 µg/ml, Bioceros BV) for 8 hours. RNA was isolated using the Aurum total RNA isolation kit (Bio-Rad) and samples were sent to ServiceXS for further microarray processing. In brief, to assess the quality of the samples, the concentration of the RNA was determined using the Nanodrop ND1000 spectrophotometer. The Agilent Bioanalyzer was used to analyze the quality and integrity of the RNA samples. The Illumina TotalPrep-96 RNA Amplification Kit was used to generate biotin labeled (biotin-16-UTP) amplified cRNA and the obtained biotinylated cRNA samples were hybridized onto the

Illumina MouseWG-6 v2 arrays. The samples were scanned using the Illumina iScan array scanner and the data retrieved using Illumina's Genomestudio v. 2011.1 software.

Microarray pre-processing and data analysis

Analyses were carried out with Bioconductor packages in the statistical software package R (version 3.1.3). Normexp-by-control background correction, quantile normalization, and log2 transformation were performed on the Illumina sample and control probe profiles using the limma package (version 3.22.7). The arrayQualityMetrics package (version 3.22.1) was used to assess whether the microarray data were of good quality. Only probes detected (detection p-value < 0.05) on at least one array were included in the differential expression analysis. Gene-wise linear models were fitted using the limma package. Differential expression between the different conditions was assessed via a moderated t-test. The illuminaMousev2.db package (version 1.24.0) was used to update the probe annotation provided by Illumina. The data set with differentially expressed genes (nominal p-value<0.05) was analyzed using Ingenuity Pathway Analysis (IPA, Ingenuity Systems) to test for enriched canonical pathways and networks. The background set for the gene enrichment analyses consisted of all genes that were detected on at least one array. Significance of enrichment was calculated using a right-tailed Fisher's Exact Test and the resulting p-values were corrected for multiple testing using the Benjamini-Hochberg false discovery rate. The microarray data have been deposited in NCBI Gene Expression Omnibus in a MIAME compliant format and are accessible under GEO Series accession number 90835 (GSE90835).

Docking Simulations

Molecular docking simulations of ligand binding to the TRAF6 C-domain were performed using Autodock Vina and binding modes were visualized and analyzed using PyMOL (www.pymol.org). The high-resolution X-ray structures of the CD40-TRAF6 complex (PDB 1LB6) was used to model the binding mode of compounds onto TRAF6. A model for monomeric TRAF6 was isolated from the .pdb files and additional molecules in the structure (ligands, detergents, H_2O) were removed. Compounds were prepared in the .pdbqt ligand file format using the AutoDock Tools (ADT) software suite. Definition of rotatable bonds allowed flexible docking and optimal orientation of target molecules to the protein. Protein structure (.pdb) files were obtained from the RCSB protein data bank (www.rcsb.org) and transformed to .pdbqt receptor files using ADT. A search space was defined by the Grid Box module in ADT.

TRAF6 C-domain mutants: expression, purification and binding analyses

The TRAF6 C-domain (residues 346-504) was carboxy-terminally His-tagged by cloning into the pET21d expression vector (Novagen). Mutants of the TRAF6 C-domain were generated by site-directed mutagenesis using the QuickChange site-directed mutagenesis method (Stratagene) according to the manufacturer's instruction. The primers used to generate the mutants are listed in Suppl. Table 3. All constructs were verified by sequencing. Recombinant TRAF6 C-domain and its mutants were overexpressed in *E. coli* BL21 (DE3) and affinity-purified using a Ni-NTA column mounted on an NGC medium pressure chromatography system (Bio-Rad). Bound protein was eluted using an imidazole gradient and the buffer was exchanged to 10 mM Hepes, pH 7.4, 150 mM NaCl and 5 mM 2-mercaptoethanol using a Bio-Gel P-6 column (Bio-Rad). The direct binding between the TRAF6 C-domain and the 6877002 and 6860766 compounds was

measured via SPR (Biacore T200, GE Healthcare). TRAF6 C-domains were immobilized on HC1500M Sensor Chips using the amine coupling method. This reached a density of approximately 37,000 RU. Compounds were dissolved in SPR running buffer (PBS, 0.05% Tween-20, 5% DMSO, pH 7.4). All measurements were carried out at 25^{o}C and with a flow rate of 50 µl min^{-1} in SPR running buffer. Sensorgrams were corrected by subtraction of the level of SPR signal observed on the empty reference flow channel during injection of the compounds. Data were analyzed using the BIAevaluation software. Equilibrium dissociation constants (K_D) were determined from a model of the steady state affinity (at least 2 independent runs performed in duplicate were averaged).

Experimental autoimmune encephalomyelitis

Experimental autoimmune encephalomyelitis (EAE) was induced in 10-week-old female C57BL/6 mice (n=11-12 per group) and immunoglobulin levels were determined, as described above. On day 0, mice were immunized subcutaneously with 200 µg of a myelin oligodendrocyte glycoprotein peptide (MOG35-55) emulsified in complete Freund's adjuvant (CFA) supplemented with 4 mg/ml M. tuberculosis H37Ra (Hooke Laboratories). Mice were injected IP on days 0 and 1 with 400 ng pertussis toxin. Mice were treated daily by IP injection with the vehicle (0.05% Tween 80, 5% DMSO in saline) or with 10 µmol/kg of 6877002 or 6860766 starting 3 days before EAE induction until 17 days after the induction of EAE. The animals were sacrificed 16 days after induction of EAE for analysis of immunoglobulin levels at the peak of the disease (n=4-6 per group) or 30 days (n=5-8 per group) after induction of EAE for analysis of immunoglobulin levels at the end of the disease.

DC-OTII co-cultures

Bone marrow cells derived from femur and tibia of C57Bl6 mice were cultured for 10 days in IMDM supplemented with 9% FBS, 100 U/ml Pen/Strep (GE Healthcare Life Sciences), 2mM Glutamin (Thermo Fisher) and 20 µM beta-mercaptoethanol (Sigma Aldrich) and 20 ng/ml GMCSF (Peprotech) at 37C and 5% CO2. 50.000 DC were plated in 96 well plates (Greiner) and pre-treated for 1 hour with 10 µM compound or vehicle. Splenic CD4 T-cells from OT-II transgenic mice were purified using negative selection according to the manufacturers' instructions (Magnisort, ebioscience) and labelled with CFSE (1 µM, 10 min, Invitrogen).

DC and OT-II were co-cultured in a 1:2 ratio with or without 1 µg/ml OVA323 (ISQAVHAAHAEINEAGR, Genscript). After 96 hours cells were collected and stained with anti-CD4-efluor450, anti-CD25-APC and anti-Thy1.2-Pe/Cy7 (all Thermofisher) and analysed with flowcytometry (CytoFlex, Beckman Coulter).

Peritonitis

E. coli peritonitis was induced in male C57BL/6 mice (n=8 per group) and bacterial outgrowth was analyzed. *E. coli* O18:K1 was cultured in Luria-Bertani medium (Difco) at 37 °C to midlog phase and washed twice with pyrogen-free sterile 0.9% NaCl (Baxter), as previously described (2). The amount of bacteria in the culture was estimated by measuring the A600 in a spectrophotometer. Mice were injected IP with 1×10^4 cfu in 200 µl of 0.9% NaCl. Serial dilutions of the final bacterial inoculum were plated on blood agar plates and incubated overnight at 37 °C to verify the amount of viable bacteria injected. Mice were treated by IP injection with the vehicle (0.05% Tween 80, 5% DMSO in saline) or with 10 µmol/kg of 6877002 or 6860766 starting 3 hours before and 6 and 12 hours after induction of perotinitis. The animals were

sacrificed 16 hours after induction of peritonitis using inhalation anesthesia with isoflurane. Peritoneal lavage was performed with 5 ml of sterile phosphate-buffered saline, blood was isolated via cardiac puncture. Liver lobes and lungs were isolated and homogenized in PBS using a tissue homogenizer (Biospec Products). Bacterial loads in peritoneal lavage fluid, blood, and tissue homogenates were determined by plating serial dilutions of each sample on blood agar plates overnight at 37 °C and counting the number of cfu.

Synthesis of rHDL based nanoparticles

The synthesis of rHDL-6877002 was based on a previously published method (3). In short, the CD40-TRAF6 inhibitor 6877002 was combined with 1-myristoyl-2-hydroxy-sn-glycero-phosphocholine (MHPC) and 1, 2-dimyristoyl-sn-glycero-3-phosphatidylcholine (DMPC) (Avanti Polar Lipids) in chloroform/methanol mixture (9:1 by volume) and then dried in a vacuum, creating a thin lipid film. Human apolipoprotein A1 (apoA-I) was dissolved in PBS and added to the lipid film. The apoA-I was left to incubate at 37°C for 1 hour or until the film was hydrated and a homogenous solution was formed. The solution was then sonicated for 20 minutes to form rHDL-6877002 nanoparticles. Subsequently, the solution was purified by multiple centrifugation and filtration steps. In targeting, imaging and biodistribution experiments, the components for rHDL-6877002 were combined with DiR or DiO (Invitrogen) to allow for incorporation of the labels.

Ex vivo near infrared fluorescence imaging (NIRF)

Female *Apoe*$^{-/-}$ mice fed a high-fat diet for 12 weeks, received a single IV injection with DiR (0.5 mg/kg) labeled rHDL-6877002 (10μmol/kg, n=3) or saline (n=1). Mice were sacrificed 24 hours

after the injection and perfused with 60 mL PBS. Liver, spleen, lung, kidneys, heart and muscle tissue were collected for NIRF imaging. Fluorescent images were acquired with the IVIS 200 system (Xenogen), with a 2 second exposure time, using a 745 nm excitation filter and a 820 nm emission filter.

Statistics

Data are presented as mean ± SEM. Data were analyzed by using either an unpaired Student's *t* test, a Bonferoni-corrected Student's *t* test, or an ANOVA as indicated, using the GraphPad Prism 5.0 software (GraphPad Software, Inc.). P-values <0.05 were considered significant.

Online Fig. 1. TRAF-STOP treatment does not induce toxicity in *Apoe*$^{-/-}$ mice with early atherosclerosis (n=12-15 per group). Bodyweight (**A**), cholesterol levels (**B**), hemoglobin concentration (**C**), platelet counts (**D**) leukocyte numbers (**E**) and leukocyte subsets (**F**) did not differ between control and TRAF-STOP treated mice. Histologic analysis of the liver (**G**) and lungs (**H**) showed no abnormalities (scale bar 100 μm).

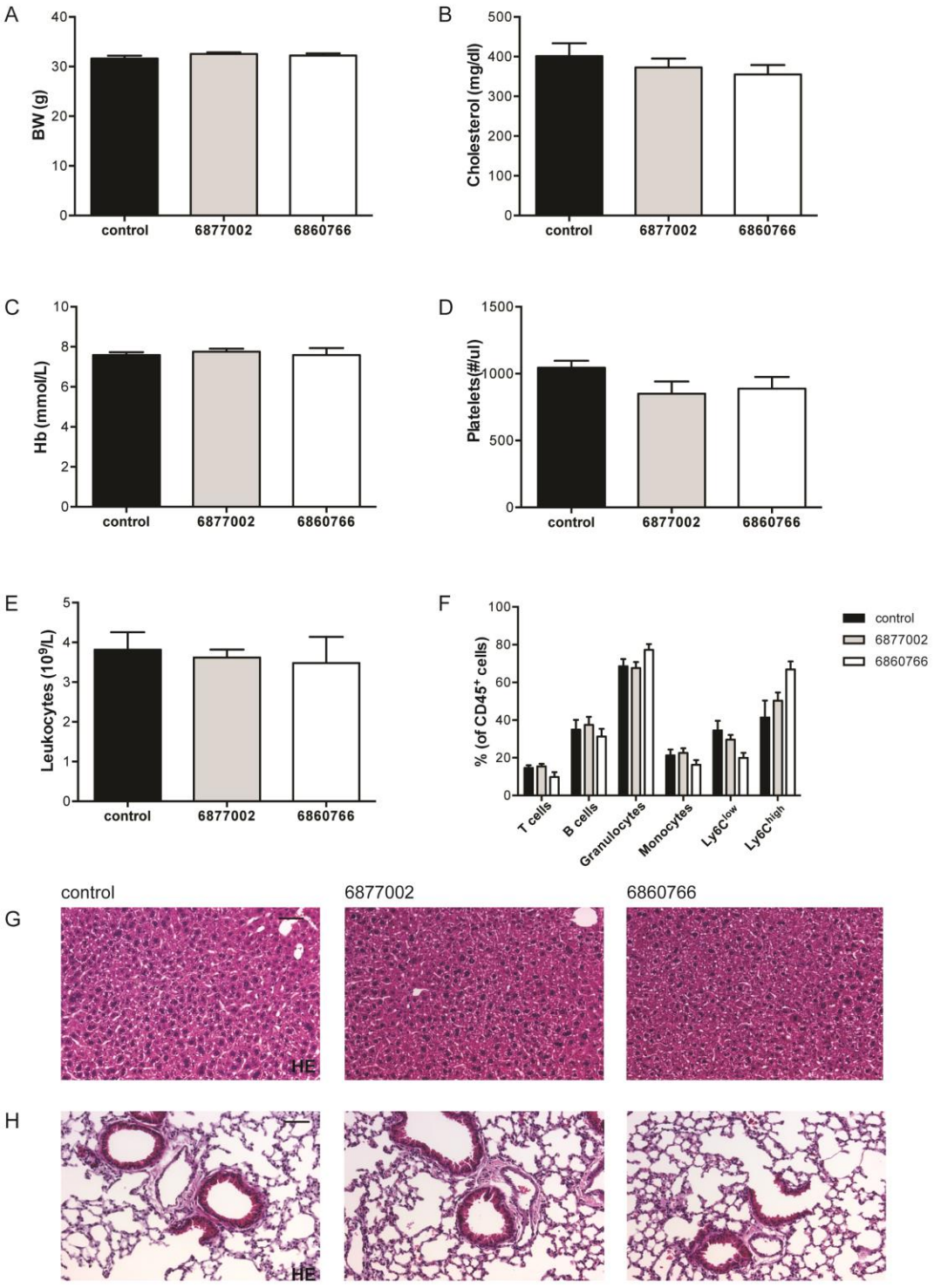
A
BW (g)
40
30
20
10
0
control
6877002
6860766
B
Cholesterol (mg/dl)
500
400
300
200
100
0
control
6877002
6860766
C
Hb (mmol/L)
10
8
6
4
2
0
control
6877002
6860766
D
Platelets(#ul)
1500
1000
500
0
control
6877002
6860766
E
Leukocytes (10^9/L)
5
4
3
2
1
0
control
6877002
6860766
F
% (of CD45+ cells)
100
80
60
40
20
0
T cells
B cells
Granulocytes
Monocytes
Ly6Clow
Ly6Chigh
control
6877002
6860766
G
control
6877002
6860766
HE
H
HE

Online Fig. 2. Plaque phenotypic characteristics after 6 weeks TRAF-STOP treatment of early atherosclerosis (n=12-15 per group). No differences in proliferation (**A**), apoptosis (**B**), collagen content (**C**) or smooth muscle content (**D**) were observed between TRAF-STOP and control treated mice.

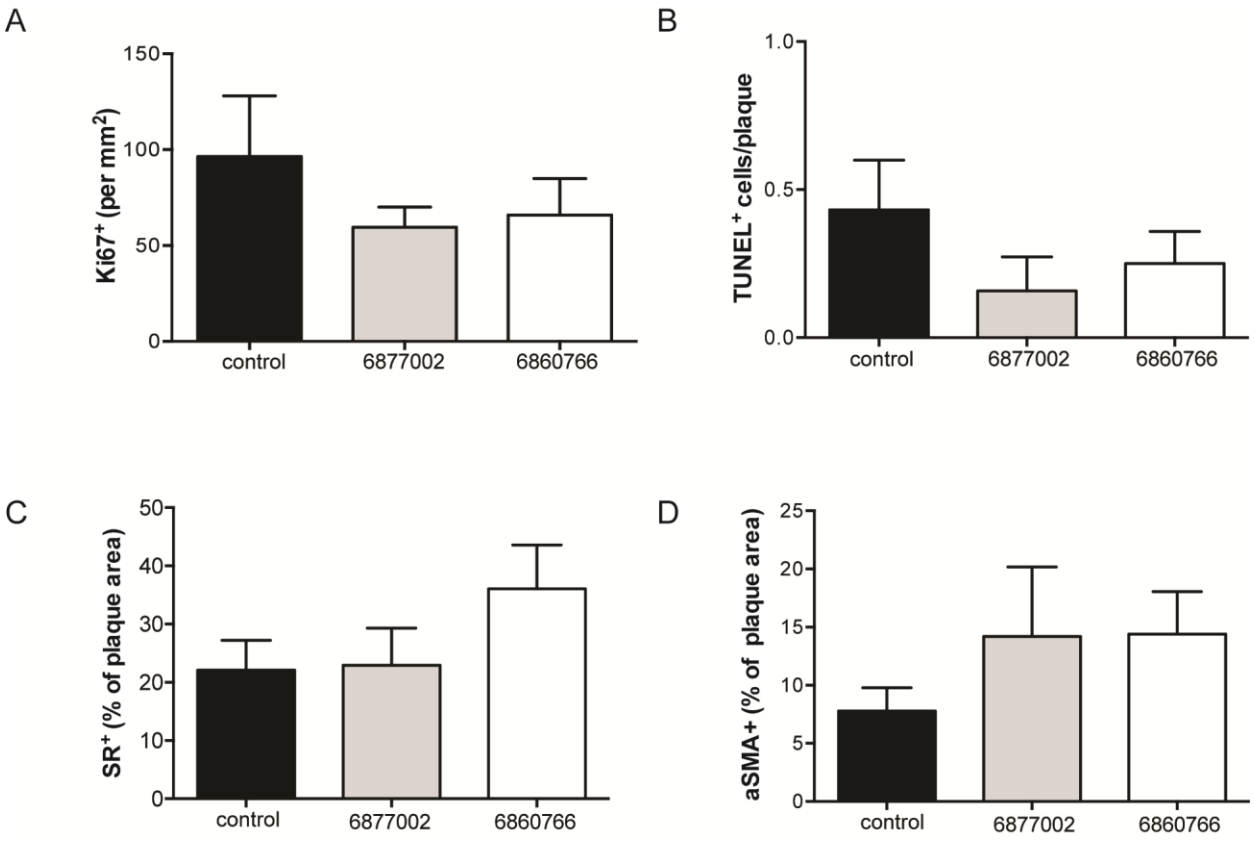

Online Fig. 3. TRAF-STOP treatment does not induce toxicity in *Apoe*$^{-/-}$ mice with established atherosclerosis (n=11-12 per group). No differences in bodyweight (**A**), cholesterol levels (**B**), hemoglobin concentration (**C**), platelet counts (**D**), leukocyte numbers (**E**) and leukocyte subsets (**F**) were observed between control and TRAF-STOP treated mice. Metabolic parameters in control and TRAF-STOP treated mice (**G-K**). TRAF-STOP did not affect ALT and AST levels (**L**). Plaque area in the aortic root drecreased upon TRAF-STOP treatment (scale bar 1 mm, n=11-12 per group) (**M**). The majority of Ki67^{+} cells (brown) in the plaques are macrophages (red). The image shows a Mac3^{+}Ki67^{+} cell (arrow) and Mac3^{-}Ki67+ cell (asterisk) in an atherosclerotic plaque in the brachiocephalic trunk (scale bar 40 μm) (**N**). *=p<0.05, ***=p>0.001, ****=p<0.0001.

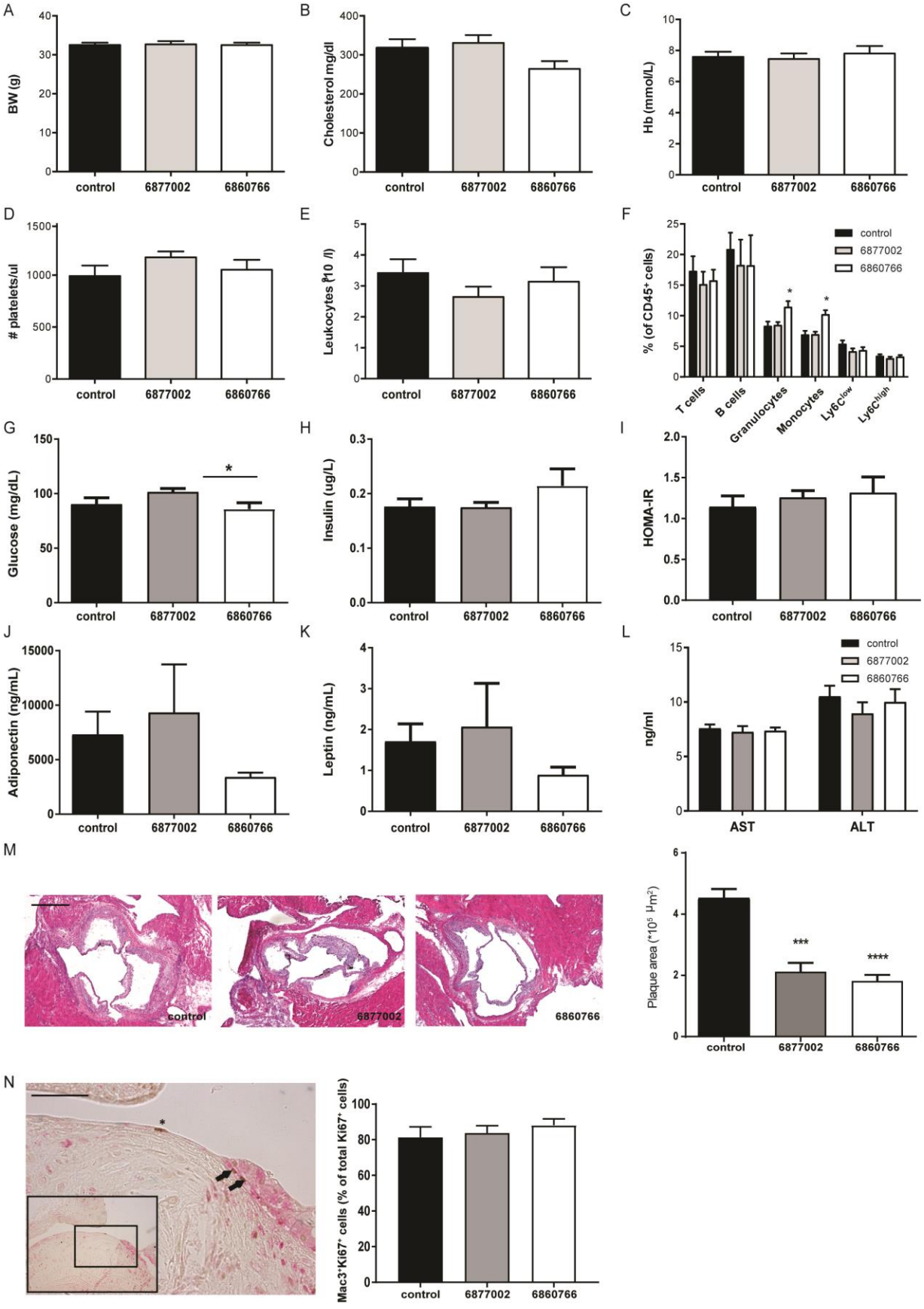
A
BW (g)
control
6877002
6860766
B
Cholesterol mg/dl
C
Hb (mmol/L)
D
platelets/ul
E
Leukocytes (10 /l)
F
% (of CD45+ cells)
control
6877002
6860766
T cells
B cells
Granulocytes
Monocytes
Ly6Clow
Ly6Chigh
G
Glucose (mg/dL)
H
Insulin (ug/L)
I
HOMA-IR
J
Adiponectin (ng/mL)
K
Leptin (ng/mL)
L
ng/ml
AST
ALT
M
Plaque area (*10^5 µm^2)
***
****
N
Mac3+Ki67+ cells (% of total Ki67+ cells)

Online Fig. 4. TRAF-STOP 6877002 induces a minor decrease in Ly6C^{low} monocytes in the spleen, T cells, B cells, granulocytes and total monocytes are not affected (n=11-12) (**A**). Bone marrow hematopoietic stem and progenitor cell populations are not affected by TRAF STOPS (n=3) (**B**). LSK: Lin$^-$Sca-1$^+$CKit$^+$; HSC: LSK CD150$^+$CD34$^-$CD48$^-$CD135$^-$; MMP1: LSK CD150$^+$CD34$^+$CD48$^-$CD135$^-$; MMP2: LSK CD150$^+$CD34$^+$CD48$^+$CD135$^-$; MMP3: LSK CD150$^-$ CD34$^+$CD48$^+$CD135$^-$; CMP: LSK CD34$^+$CD16/32$^-$; GMP: LSK CD34$^+$CD16/32$^+$; MEP LSK CD34$^-$CD16/32$^-$.*=*p<0.05.*

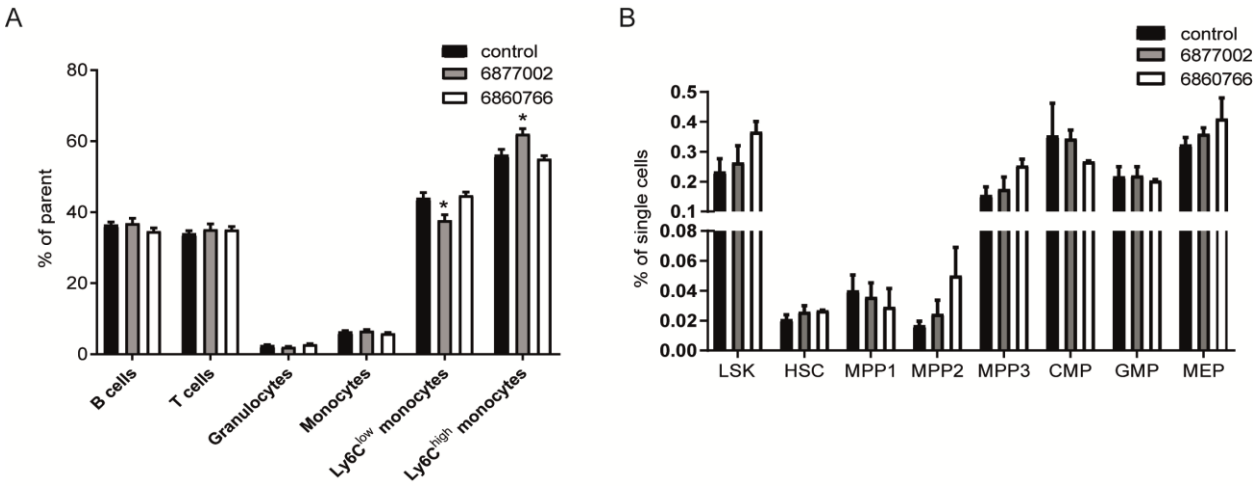

Online Fig. 5. TRAF-STOPs do not affect phagocytosis (**A**) or efferocytosis (**B**) or the expression of ABC transporters (**C**) (n=8).

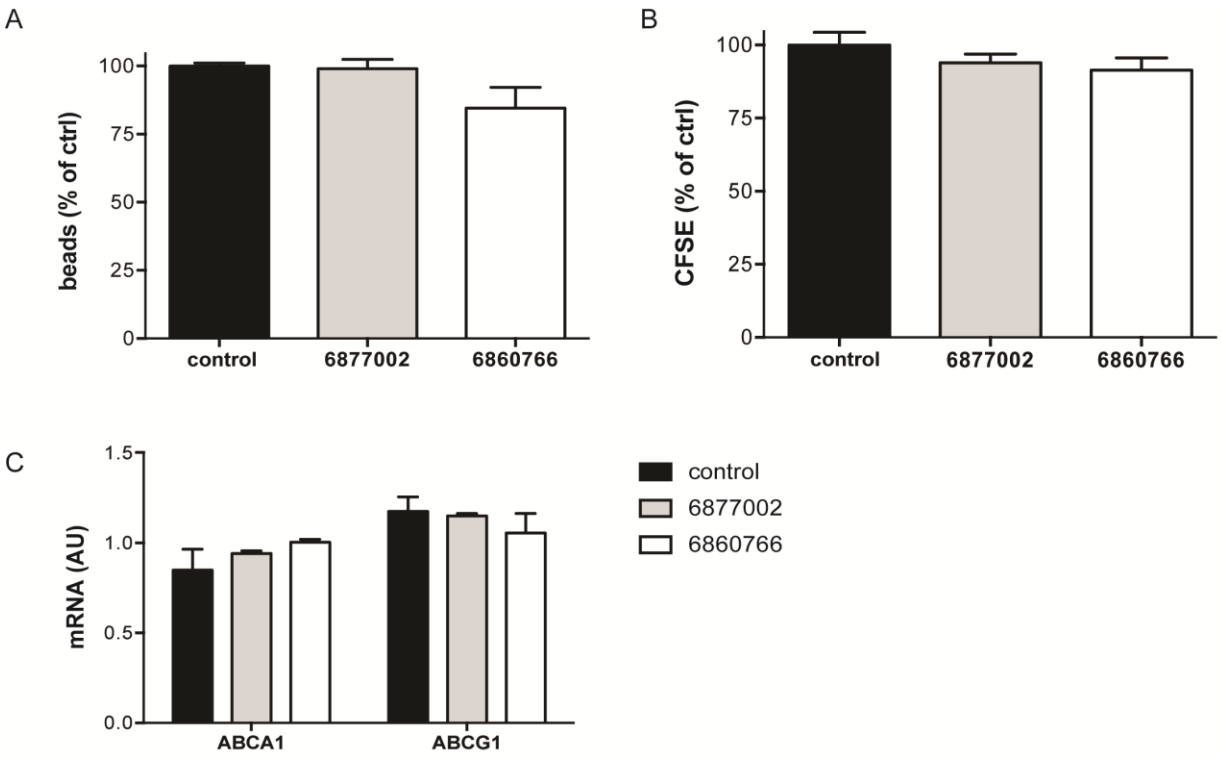

Online Fig. 6. Transcriptomics analysis of bone marrow-derived macrophages. Graphs represent triplicates and are representative examples of 3 independent experiments. Networks of the top 25 canonical pathways as identified by IPA (Suppl. Table 1 & 2) with at least 4 genes in common were generated and revealed that TRAF-STOP 6860766 has a profound effect on cholesterol synthesis and immune response (**A**) and that TRAF-STOP 6877002 in addition also affects cell cycle progression (**B**). Overview of the TRAF-STOP-induced alterations in cholesterol biosynthesis pathways (**C, D**). TRAF-STOP 6877002 affects mRNA expression of cell cycle related genes (n=3) (**E**). *=$p < 0.05$

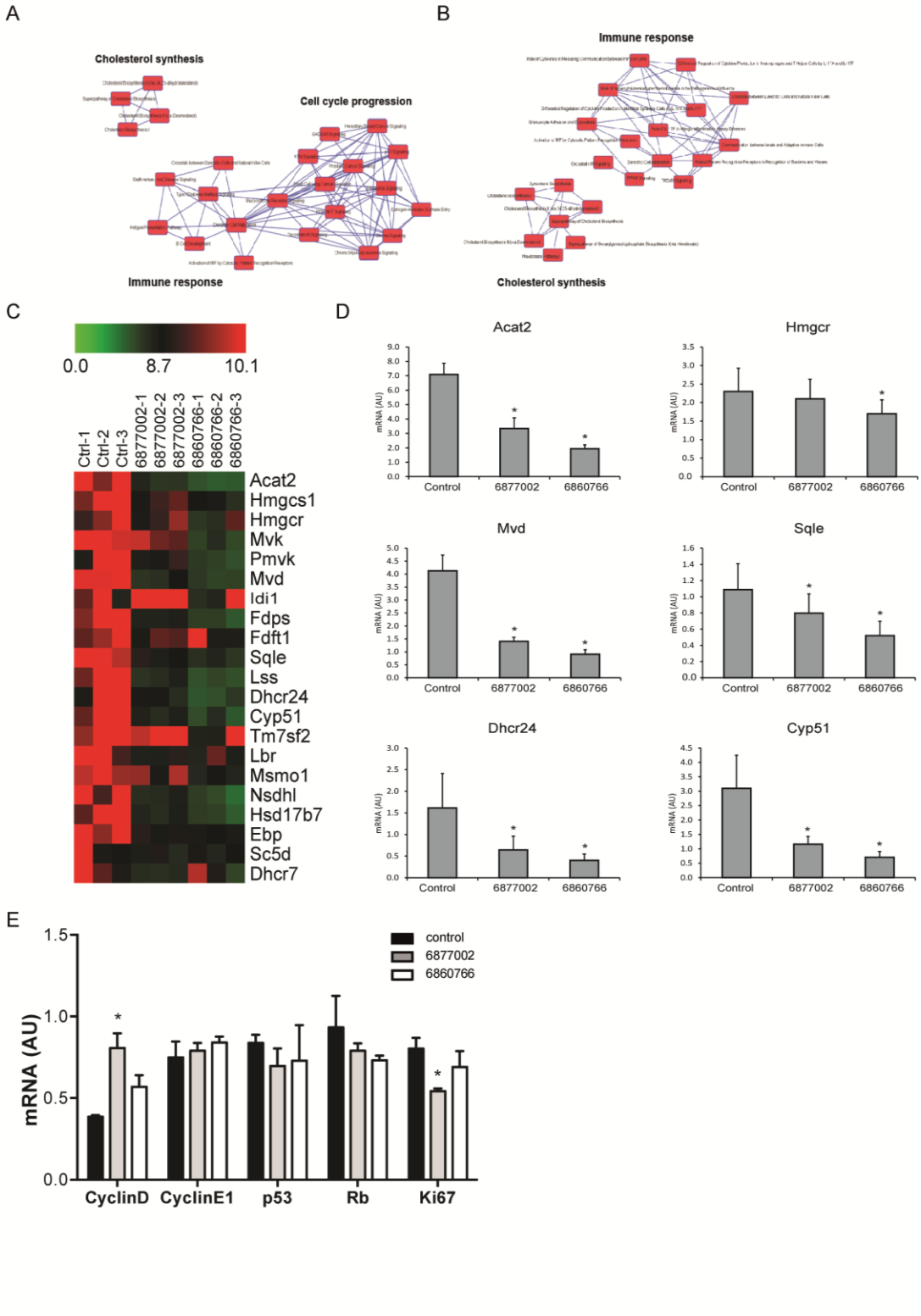
A
Cholesterol synthesis
Cell cycle progression
Immune response
B
Immune response
Cholesterol synthesis
C
0.0
8.7
10.1
Ctrl-1
Ctrl-2
Ctrl-3
6877002-1
6877002-2
6877002-3
6860766-1
6860766-2
6860766-3
Acat2
Hmgcs1
Hmgcr
Mvk
Pmvk
Mvd
Idi1
Fdps
Fdft1
Sqle
Lss
Dhcr24
Cyp51
Tm7sf2
Lbr
Msmo1
Nsdhl
Hsd17b7
Ebp
Sc5d
Dhcr7
D
Acat2
Hmgcr
Mvd
Sqle
Dhcr24
Cyp51
mRNA (AU)
Control
6877002
6860766
E
control
6877002
6860766
mRNA (AU)
CyclinD
CyclinE1
p53
Rb
Ki67

Online Fig. 7. TRAF-STOP 6877002 and 6860766 bind differently to TRAF6. Molecular surface of the TRAF6 C-domain (green, PDB ID: 1LB6) in complex with a CD40 peptide fragment (**A**) and with 6877002 (in pink) and 6860766 (in blue) as predicted by molecular docking experiments (**B**). The drugable pocket is colored in yellow and the newly identified residues involved in binding of the TRAF-STOPs are colored in blue. Computer modeling has predicted interaction of TRAF-STOPs with residues His376 and Arg466 (via π-π stacking and π-cation interaction) (4), therefore these residues were mutated into alanine residues to prevent the interaction. Surface plasmon resonance (SPR) experiments confirmed that TRAF-STOP 6877002 binds to the C-domain of TRAF6 with a K_D value of 45 μM, however mutation of His376 or Arg466 into an Ala residue did not affect the binding of TRAF-STOP 6877002 to the TRAF6 C-domain. To further identify residues of the TRAF6 C-domain that could interact with the TRAF-STOPs, we performed molecular docking simulations of 6877002 and 6860766 binding to TRAF6. These analyses identified residues Lys469 and Val474 as potential interaction sites. (**C**) SPR Direct Binding of TRAF-STOP 6877002 to mutants of the TRAF6 C-domain. Mutation of Val474 into a serine residue did not affect binding of TRAF-STOP 6877002 to the TRAF6 C-domain, whereas, mutation of Lys469 into an alanine residue significantly decreased the binding of this TRAF-STOP. (**D**) For TRAF-STOP 6860766, the reverse was true: only mutation of Val474 into a serine residue affected binding to the TRAF6 C-terminus.

A

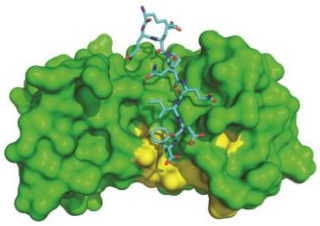

B

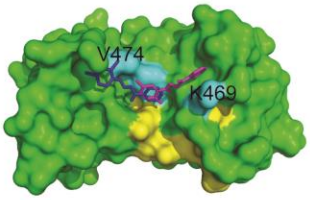

C 6877002

TRAF6 C-domain	K_d (μM)
WT	45
H376A	38
R466A	48
K469A	132
V474S	44

D 6860766

TRAF6 C-domain	K_d (μM)
WT	11
H376A	12
R466A	12
K469A	12
V474S	16

Online Fig. 8. Six week rHDL-6877002 treatment does not induce toxicity in *Apoe*$^{-/-}$ mice with early atherosclerosis. Bodyweight (**A**) was not affected. A minor increase in cholesterol levels was observed in rHDL-6877002 treated mice (**B**). Hemoglobin concentration (**C**) and platelets counts (**D**) were not affected. A slight increase in leukocyte numbers was observed in rHDL-6877002 treated mice (**E**), but relative numbers of leukocyte subsets were not altered (**F**). No signs of hepatotoxicty were observed in rHDL-6877002 treated mice. HE staining, CD45 immunohistochemistry and sirius red staining revealed no inflammation or fibrosis in the liver (scale bar 100 μm) (**G**). ALT and AST levels were not affected by rHDL-6877002 treatment (**H**). Analysis of splenic leukocyte subsets by flow cytometry revealed no abnormalities and rHDL-6877002 treatment did not affect immunoglobulin levels (**I,J**) (n=5-6).

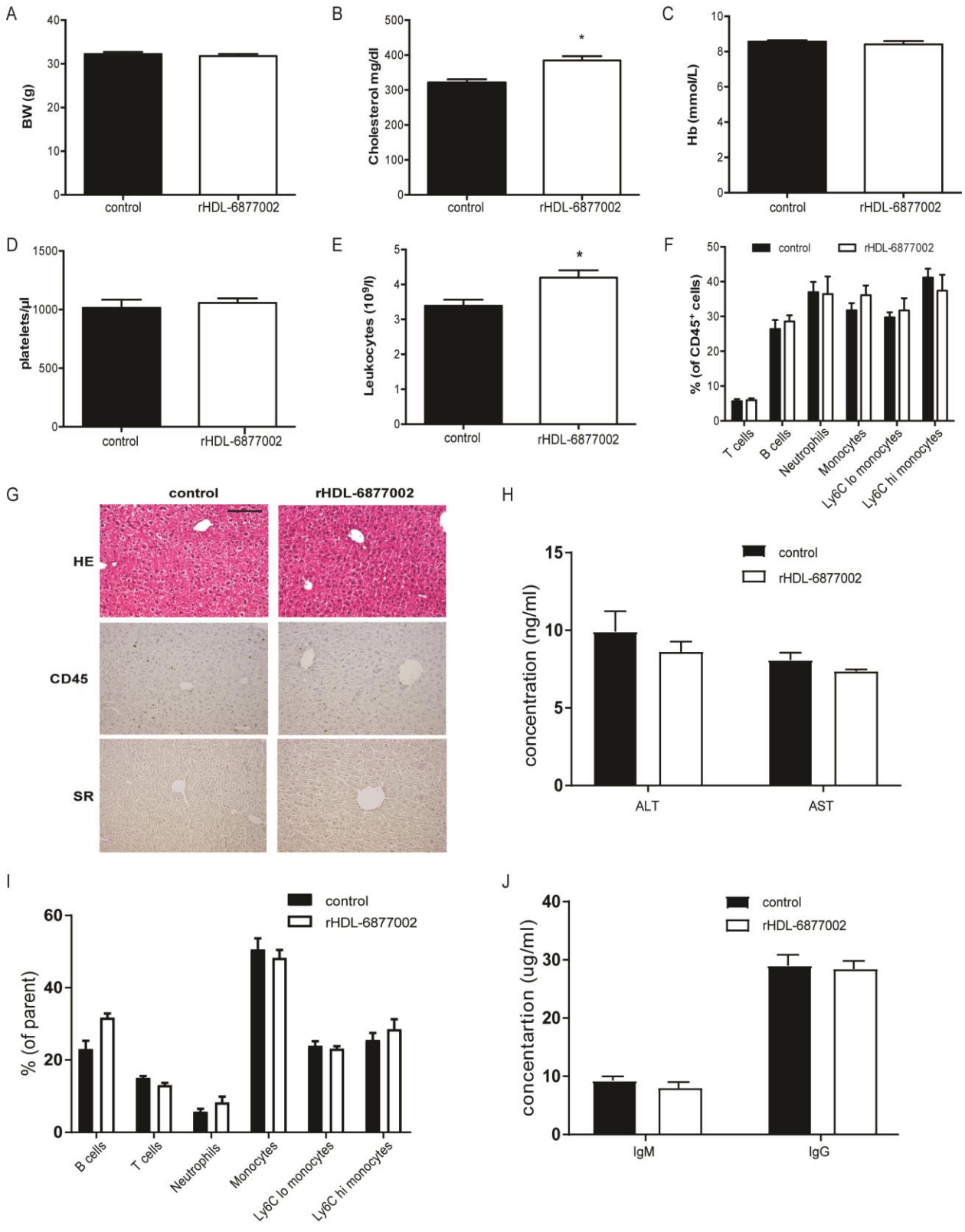
A
BW (g)
control
rHDL-6877002
B
Cholesterol mg/dl
*
C
Hb (mmol/L)
D
platelets/µl
E
Leukocytes (10^9/l)
F
% (of CD45+ cells)
T cells
B cells
Neutrophils
Monocytes
Ly6C lo monocytes
Ly6C hi monocytes
G
HE
CD45
SR
H
concentration (ng/ml)
ALT
AST
I
% (of parent)
J
concentartion (ug/ml)
IgM
IgG

References

1. Lutgens E, Lievens D, Beckers L, et al. Deficient CD40-TRAF6 signaling in leukocytes prevents atherosclerosis by skewing the immune response toward an antiinflammatory profile. The Journal of experimental medicine. 2010;207(2):391-404.
2. 't Veer C, van den Pangaart PS, Kruijswijk D, Florquin S, de Vos AF, van der Poll T. Delineation of the role of Toll-like receptor signaling during peritonitis by a gradually growing pathogenic Escherichia coli. l Chem. 2011 Oct 21;286(42):36603-18.
3. Duivenvoorden R, Tang J, Cormode DP, et al. A statin-loaded reconstituted high-density lipoprotein nanoparticle inhibits atherosclerotic plaque inflammation. Nature communications. 2014;5:3065.
4. Zarzycka B, Seijkens T, Nabuurs SB, et al. Discovery of small molecule CD40-TRAF6 inhibitors. Journal of chemical information and modeling. 2015;55(2):294-307.

Online Table 1. Top 25 canonical pathways associated with differentially expressed genes in 6877002-treated vs control-treated BMDMs

IPA canonical pathway	P-value	Adjusted p-value	Ratio	Z-score
Cholesterol Biosynthesis I	2.14E-07	3.63E-05	0.75	n/a
Cholesterol Biosynthesis II (via 24,25-dihydrolanosterol)	2.14E-07	3.63E-05	0.75	n/a
Cholesterol Biosynthesis III (via Desmosterol)	2.14E-07	3.63E-05	0.75	n/a
Superpathway of Cholesterol Biosynthesis	3.39E-06	3.09E-04	0.46	n/a
Antigen Presentation Pathway	3.39E-06	3.09E-04	0.46	n/a
Prostate Cancer Signaling	3.55E-06	3.09E-04	0.29	n/a
Melanoma Signaling	9.77E-06	7.24E-04	0.36	n/a
Dendritic Cell Maturation	2.45E-05	0.002	0.22	n/a
ATM Signaling	6.31E-05	0.003	0.29	-1.732
Estrogen-mediated S-phase Entry	6.61E-05	0.003	0.42	-1.667
Activation of IRF by Cytosolic Pattern Recognition Receptors	1.02E-04	0.005	0.30	1.807
p53 Signaling	1.07E-04	0.005	0.24	0.258
B Cell Development	1.82E-04	0.007	0.41	n/a
Small Cell Lung Cancer Signaling	2.34E-04	0.009	0.25	n/a
Type I Diabetes Mellitus Signaling	2.88E-04	0.010	0.23	0.333
Oncostatin M Signaling	3.09E-04	0.010	0.33	n/a
GADD45 Signaling	3.31E-04	0.010	0.42	n/a
PI3K/AKT Signaling	3.55E-04	0.010	0.21	0.626
Glucocorticoid Receptor Signaling	3.98E-04	0.011	0.17	n/a
Graft-versus-Host Disease Signaling	3.98E-04	0.011	0.32	n/a
Chronic Myeloid Leukemia Signaling	7.08E-04	0.017	0.22	n/a
Hereditary Breast Cancer Signaling	9.77E-04	0.022	0.20	n/a
Assembly of RNA Polymerase I Complex	0.001	0.022	0.56	n/a
Crosstalk between Dendritic Cells and Natural Killer Cells	0.001	0.022	0.24	n/a
Glioma Signaling	0.001	0.026	0.21	-0.728

Statistical significance was determined by using Fisher's exact test ($P < 0.05$) and were adjusted for multiple testing using the Benjamini-Hochberg false discovery rate.

Online Table 2. Top 25 canonical pathways associated with differentially expressed genes in 6860766-treated vs control-treated BMDMs

IPA canonical pathway	P-value	Adjusted p-value	Ratio	Z-score
Superpathway of Cholesterol Biosynthesis	2.69E-09	1.38E-06	0.54	n/a
Cholesterol Biosynthesis I	8.32E-07	1.05E-04	0.67	n/a
Cholesterol Biosynthesis II (via 24,25-dihydrolanosterol)	8.32E-07	1.05E-04	0.67	n/a
Cholesterol Biosynthesis III (via Desmosterol)	8.32E-07	1.05E-04	0.67	n/a
Interferon Signaling	1.10E-05	0.001	0.38	-2.111
Zymosterol Biosynthesis	2.24E-05	0.002	0.83	n/a
Antigen Presentation Pathway	2.40E-05	0.002	0.39	n/a
TREM1 Signaling	3.02E-05	0.002	0.25	-2.183
Activation of IRF by Cytosolic Pattern Recognition Receptors	3.89E-05	0.002	0.28	-1.604
Mismatch Repair in Eukaryotes	1.62E-04	0.002	0.25	-2.183
Role of Hypercytokinemia/hyperchemokinemia in the Pathogenesis of Influenza	2.24E-04	0.010	0.33	n/a
Differential Regulation of Cytokine Production in Intestinal Epithelial Cells by IL-17A and IL-17F	2.51E-04	0.011	0.41	n/a
Dendritic Cell Maturation	3.72E-04	0.015	0.17	n/a
Granulocyte Adhesion and Diapedesis	4.68E-04	0.016	0.17	n/a
Communication between Innate and Adaptive Immune Cells	4.68E-04	0.016	0.23	n/a
GADD45 Signaling	5.62E-04	0.018	0.37	n/a
Differential Regulation of Cytokine Production in Macrophages and T Helper Cells by IL-17A and IL-17F	8.51E-04	0.026	0.40	n/a
Crosstalk between Dendritic Cells and Natural Killer Cells	0.001	0.030	0.21	n/a
Oncostatin M Signaling	0.001	0.031	0.27	-1.414
Superpathway of Geranylgeranyldiphosphate Biosynthesis I (via Mevalonate)	0.001	0.032	0.38	n/a
Role of Pattern Recognition Receptors in Recognition of Bacteria and Viruses	0.001	0.033	0.17	-2.333
Mevalonate Pathway I	0.002	0.045	0.42	n/a
PPAR Signaling	0.002	0.045	0.18	1.500
Role of Cytokines in Mediating Communication between Immune Cells	0.002	0.045	0.25	n/a
Role of IL-17F in Allergic Inflammatory Airway Diseases	0.002	0.045	0.25	n/a

Statistical significance was determined by using Fisher's exact test ($P < 0.05$) and were adjusted for multiple testing using the Benjamini-Hochberg false discovery rate.

Online Table 3. Primers used to generate TRAF6C mutants.

Mutant	Primers
TRAF6C H376A	5’-GAAACCTGTTGTGATT**GCT**AGCCCTGGATTCTAC-3’
	5’-GTAGAATCCAGGGCT**AGC**AATCACAACAGGTTTC-3’
TRAF6C R466A	5’-GCGACCCACAATCCCA**GCT**AACCCAAAAGGTTTTGGC-3’
	5’-GCCAAAACCTTTTGGGTT**AGC**TGGGATTGTGGGTCGC-3’
TRAF6C K469A	5’-AATCCCACGGAACCC<u>T</u>**GCA**GGTTTTGGCTATG-3’
	5’-CATAGCCAAAACC**TGC**<u>A</u>GGGTTCCGTGGGATT-3’
TRAF6C V474S	5’-CCCAAAAGGTTTTGGCTAT**AGT**ACTTTTATGCATCTGGAAGCC-3’
	5’- GGCTTCCAGATGCATAAAAGT**ACT**ATAGCCAAAACCTTTTGGG-3’

The bold nucleotides encode the mutated amino acids. The underlined nucleotides are silent mutation introducing a restriction site.